

# Combined Quantum-Mechanical Molecular Mechanics Calculations with NWChem and AMBER: Excited State Properties of Green Fluorescent Protein Chromophore Analogue in Aqueous Solution

Teerapong Pirojsirikul,<sup>[a]</sup> Andreas W. Götz,<sup>[b]</sup> John Weare,<sup>[a]</sup> Ross C. Walker,<sup>[a,c]</sup> Karol Kowalski,<sup>[d]</sup> and Marat Valiev <sup>[d]</sup>

Combined quantum mechanical molecular mechanics (QM/MM) calculations have become a popular methodology for efficient and accurate description of large molecular systems. In this work we introduce our development of a QM/MM framework based on two well-known codes—NWChem and AMBER. As an initial application area we are focused on excited state properties of small molecules in an aqueous phase using an analogue of the green fluorescent protein (GFP) chromophore as a particular test case. Our approach incorporates high level coupled cluster theory for the analysis of excited states providing a reliable theoretical analysis of effects of an aqueous solvation environment on the photochemical properties of the GFP chromophore. Using a systematic approach, which involves comparison of gas phase and aqueous phase results for different protonation states and

conformations, we resolve existing uncertainties regarding the theoretical interpretation of experimental data. We observe that the impact of aqueous environment on charged states generally results in blue shifts of the absorption spectra, but the magnitude of the effect is sensitive to both protonation state and conformation and can be rationalized based on charge movement into the area of higher/lower external electrostatic potentials. At neutral pH levels the experimentally observed absorption signal is most likely coming from the phenol protonated form. Our results also show that the high level electron correlated method is essential for a proper description of excited states of GFP. © 2017 Wiley Periodicals, Inc.

DOI: 10.1002/jcc.24804

## Introduction

The combined quantum mechanics molecular mechanics (QM/MM)<sup>[1–4]</sup> approach provides one of the simplest examples of a multiphysics methodology for the simulation of large systems. While it has been used successfully in a number of important applications there remains a significant barrier toward utilization of QM/MM methods in the general scientific community. Part of this problem can be found in the shortage of efficient, extensible, and readily accessible implementations of the methodology that can take advantage of existing highly supported software capabilities for quantum mechanical and molecular mechanics simulations. This is the issue that we are addressing in our work through the development of a generic QM/MM interface between two well-known community codes—NWChem<sup>[5]</sup> and AMBER.<sup>[6,7]</sup> In this article, we report on the use of this interface for the description of aqueous systems, using an analogue of the green fluorescent protein (GFP) chromophore as an example application.

GFP<sup>[8]</sup> is a small protein, which is used extensively as a biomarker for gene expression and protein targeting.<sup>[9]</sup> This widespread adoption of GFP stems from its unique photo-physical properties. It consists of a chromophore derived from an autocatalytic posttranslational cyclization among three amino acid residues, Ser65, Tyr66, and Gly67.<sup>[10–19]</sup> The fluorescence is in the green region of the spectrum and pronounced when the chromophore covalently attached to the protein matrix. The

latter ensures stability of the signal, which is important for imaging applications.<sup>[20]</sup> The protein environment plays a key role in regulating the photo-physical properties of GFP.<sup>[21]</sup> This is strongly supported by the inability of GFP chromophore analogues to fluoresce in solutions.<sup>[22,23]</sup> Additionally, since the

[a] T. Pirojsirikul, J. Weare, R. C. Walker

Department of Chemistry and Biochemistry, University of California San Diego, 9500 Gilman Drive, La Jolla, California 92093

[b] A. W. Götz

San Diego Supercomputer Center, University of California San Diego, 9500 Gilman Drive, La Jolla, California 92093

[c] R. C. Walker

GlaxoSmithKline, 1250 S. Collegeville Road, Collegeville, Pennsylvania 19426

[d] K. Kowalski, M. Valiev

Environmental Molecular Sciences Laboratory, Pacific Northwest National Laboratory, P. O. Box 999, Richland, Washington 99352

E-mail: marat.valiev@pnnl.gov

Contract grant sponsors: Division of Chemical Sciences, Geosciences, and Biosciences, Office of Basic Energy Sciences, U. S. Department of Energy (DOE) (M.V.), Contract grant Sponsor EMSL, a national scientific user facility sponsored by DOE's Office of Biological and Environmental Research and located at Pacific Northwest National Laboratory, which is operated by Battelle Memorial Institute for the DOE (T.P.) and (K.K.); Contract grant sponsor: Intel Corp and Exxact Corp (R. C. W.); Contract grant sponsor: Alliance for Sustainable Energy, LLC, Managing and Operating Contractor for the National Renewable Energy Laboratory for the DOE (A.W.G.) Contract grant number: DE-AC36-99GO-10337 (A.W.G.); Contract grant sponsor: National Science Foundation; Contract grant number: CHE-1416571

© 2017 Wiley Periodicals, Inc.

discovery of wild-type GFP (wtGFP), a number of mutant GFP structures have been engineered that contain the same chromophore but exhibit different photo-physical properties.<sup>[11,24–27]</sup> All these results point to the possibility for a rational design of GFP-like systems with desired properties through targeted changes in the protein environment. A fundamental understanding of GFP chromophore chemistry and its interactions with the protein matrix would be highly beneficial to the success of such efforts.

A natural starting point toward this goal can be found in studies of model GFP chromophores, such as the *p*-hydroxybenzylidene-imidazolidinone (HBDI) molecule. The analysis of HBDI in gas phase, cluster, and bulk aqueous environments provides a unique way to isolate intrinsic chemical properties of the GFP chromophore and track the impact of the environment in a controlled manner. One important question that can be addressed in these studies is how different protonation states of the chromophore impact the excited state properties. It is known that the absorption spectrum of the wtGFP, which has a strong A-band at 395 nm and the minor B-band at 477 nm, comes from two chemically distinct chromophore states. An increase in the pH level (~11–12) reduces the intensity of the A-band and enhances the low energy B-band at 470 nm.<sup>[28]</sup> This suggests that the two bands are associated with neutral protonated and anion deprotonated states of the GFP chromophore.<sup>[29–31]</sup> It has also been proposed that a doubly protonated cation state could be present in GFP.<sup>[32]</sup> While probably unlikely in the wtGFP, such a possibility cannot be ruled out in the mutants of GFP. The important point here is that the protein environment has the capacity to control the protonation state of the chromophore, and proton transfer plays a critical role in controlling fluorescence properties of GFP.

The structural characteristics of the chromophore represent another important factor that can affect its spectroscopic properties. In either charge state (cation/neutral/anion/zwiterion) the chromophore can be found in a *cis* or *trans* conformation. The protein matrix restricts chromophore configuration enhancing fluorescence and preventing energy dissipation through internal conversion (IC). In aqueous solutions such conformational restrictions are greatly reduced, which is thought to be the main reason for fluorescence suppression.

Experimental studies of GFP chromophore analogues such as HBDI in gas phase and aqueous solutions establish useful limits on the expected absorption spectrum and anticipated changes on solvation. In the case of a cationic state the introduction of the aqueous environment results in a blue shift of the absorption spectrum of 3.05 eV<sup>[33]</sup> in gas phase to 3.13–3.20 eV<sup>[32–35]</sup> in aqueous solution. A similar effect is observed for the anion. There is, however, uncertainty in the actual value of the shift given several different estimates of the gas phase absorption values—2.59–2.84 eV.<sup>[32–36]</sup> Experimental data for the neutral state is suggestive of a red shift, but the situation is not entirely clear. In gas phase the absorption value extrapolated from Kamlet–Taft fit by Dong et al. was determined to be 3.51 eV.<sup>[32]</sup> However, the charged group technique by Rajput et al. places it at 3.35 eV for the neutral form.<sup>[37]</sup> Recently, Greenwood et al. have applied an alternative method and reported a new maximum absorption

value of the neutral form to be 3.65 eV.<sup>[38]</sup> In aqueous phase the absorption value was determined to be 3.33–3.35 eV.<sup>[32–35]</sup> Overall the available experimental data for HBDI provide an important reference point for detailed analysis of GFP photochemistry.

Theoretical studies have been instrumental in the analysis of the GFP chromophore and its analogues.<sup>[39–60]</sup> While a lot of efforts have been put into these calculations using several model chromophores and various protonation states in the gas phase, this is not the case in the aqueous solution. Despite a number of calculations reported in the aqueous phase,<sup>[49,51,56,59,61–65]</sup> the same analysis across all relevant protonation states and conformers remains incomplete. Our work contributes to these efforts by providing a systematic study among all relevant protonation states and conformers of the chromophore (HBDI) in gas phase and aqueous solution. Such study enables comparative analysis of excited states of various forms of the chromophore as a function of the environment and is important in understanding properties of the wtGFP and its mutants.

This type of analysis is difficult to accomplish using currently available computational data due to the large variations in calculated absorption values that are highly sensitive to the theoretical methodology. For example, for the neutral state in gas phase the semiempirical models predict the absorption in a range of 2.77–3.65 eV,<sup>[45,54,55,58]</sup> TD-DFT gives a range of 2.89–3.54 eV,<sup>[47,53,59,60]</sup> and correlated methods 2.88–3.69 eV.<sup>[37,43,44,50,53,60]</sup> Similar variations can be found in theoretical estimates for other GFP states. There is growing evidence that the accurate excited state description of the GFP chromophore requires explicit treatment of correlation effects. To address this issue, our excited state description relies on the completely renormalized EOMCCSD(T) approach (CR-EOMCCSD(T)), which further improves on the high level EOMCCSD (Equation-of-motion CC with singles and doubles) approach by adding correction due to triple excitations.<sup>[44]</sup>

Another important consideration is related to the solvent description. Commonly utilized continuum solvent models cannot properly capture directional hydrogen bonding effects<sup>[66]</sup>—an important factor for both aqueous and protein phases. To address this problem, one needs to introduce explicit description of solvent degrees of freedom, which can be accomplished in a number of different ways. Our QM/MM framework focuses solely on interfacing with the standard AMBER force field.<sup>[67]</sup> QM/MM methodologies based on empirical force fields have been proven to be a powerful tool in photophysical studies of the GFP chromophore or its variants in protein environment.<sup>[51,64,65,68–76]</sup> It should be noted that other approaches are possible, such as those based on effective fragment potential (EFP)<sup>[77,78]</sup> models. The EFP-based method has been employed in a recent study by Ghosh et al.<sup>[62]</sup> to determine solvatochromic shifts for the anionic form of a halogen-substituted HBDI model chromophore, 3,5-difluoro 4-hydroxybenzylidene imidazolinone (DFHBDI) in bulk aqueous phase. Our studies yield similar results for the relevant anionic HBDI species, indicating that simple QM/MM models provide a good starting point for the analysis of GFP chromophore analogues in aqueous solution. Our study also represents validity for the use of newly implemented algorithm via NWChem-AMBER interface in a condensed phase simulation.

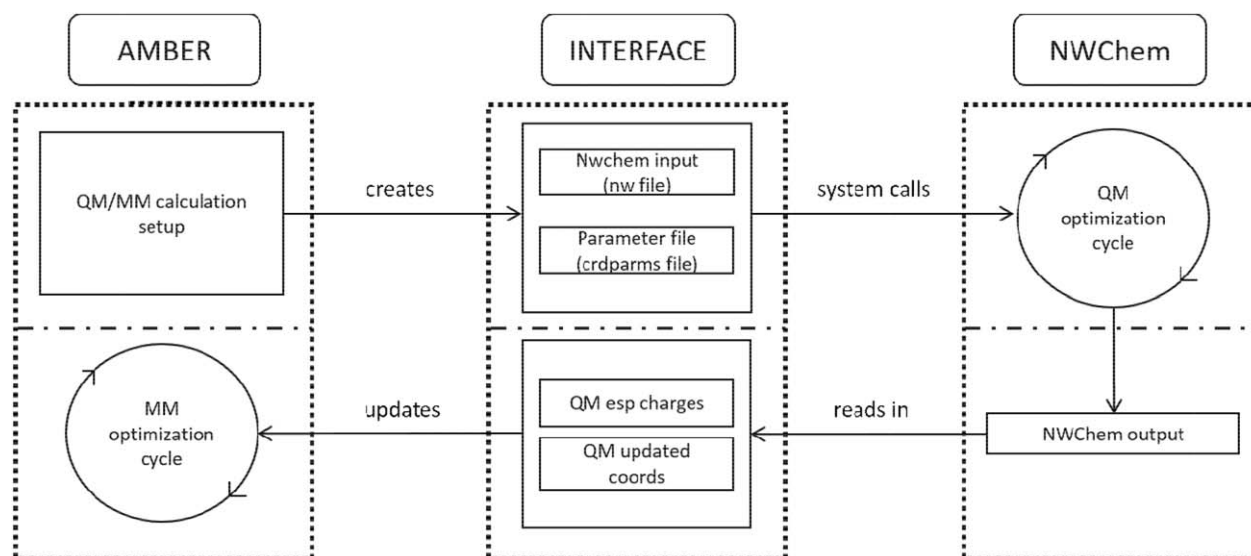


Figure 1. Diagram for a single cycle of multiregion optimization using the AMBER/NWChem interface.

## Computational Methodology and System Setup

### Gas phase

All quantum-mechanical calculations were performed using the NWChem computational chemistry code.<sup>[5]</sup> For all eight model chromophores (see Fig. 2) the optimizations were performed using density functional theory (DFT)<sup>[79–81]</sup> with the B3LYP exchange-correlation functional<sup>[82,83]</sup> and the 6-31G\* basis set.<sup>[84]</sup> The excitation energies for the optimized chromophore structures were calculated using the CR-EOMCCSD(T) method<sup>[44]</sup> with the Def2-TZVP basis set.<sup>[85]</sup> The CR-EOMCCSD(T) formalism<sup>[86–88]</sup> provides perturbative extension of the excited-state EOMCCSD method (EOMCC with singles and doubles)<sup>[89,90]</sup> to include the effect of triple excitation in a noniterative manner. In the CR-EOMCCSD(T) approach the excitation energy ( $\omega_K^{\text{CR-EOMCCSD(T)}}$ ) of the  $K$ th state is calculated as a sum of EOMCCSD excitation energy ( $\omega_K^{\text{EOMCCSD}}$ ) and a noniterative correction ( $\delta_K^{\text{CR-EOMCCSD(T)}}$ ) which captures correlation effects due to collective 3-body excitations, that is,

$$\omega_K^{\text{CR-EOMCCSD(T)}} = \omega_K^{\text{EOMCCSD}} + \delta_K^{\text{CR-EOMCCSD(T)}}. \quad (1)$$

The  $\delta_K^{\text{CR-EOMCCSD(T)}}$  is expressed in terms of triply excited moments of the EOMCCSD equations and trial function, which includes single, double, and triple excitations. The triple amplitudes of the trial wavefunction are expressed perturbatively through the EOMCCSD amplitudes. The theoretical and implementation details of this formalism have been widely discussed in the literature and we refer readers to Refs. [86–88] for more details. Recent benchmark calculations with the CR-EOMCCSD(T) formalisms<sup>[91]</sup> performed for 28 medium-size organic molecules have demonstrated that CR-EOMCCSD(T) noniterative triples corrections to the EOMCCSD excitation energies provide significant improvements to the EOMCCSD estimations, while closely matching the results of the iterative

and considerably more expensive CC3 and EOMCCSDT-3 calculations and their CASPT2 counterparts.

### Aqueous phase

Aqueous phase calculations utilized a QM/MM model where the total energy of a system is represented as

$$E_{\text{total}} = E_{\text{QM}} + E_{\text{MM}} + E_{\text{QM/MM}}, \quad (2)$$

where  $E_{\text{QM}}$  is the quantum mechanical energy of the QM subsystem,  $E_{\text{MM}}$  the molecular mechanical interactions of the MM subsystem, and  $E_{\text{QM/MM}}$  the interactions between the QM subsystem and the MM subsystem. The QM/MM interactions can be divided into two terms:

$$E_{\text{QM/MM}} = E_{\text{QM/MM}}^{\text{electrostatics}} + E_{\text{QM/MM}}^{\text{vdW}}. \quad (3)$$

The electrostatic term describes Coulomb interactions between QM and MM regions,

$$E_{\text{QM/MM}}^{\text{electrostatics}} = - \sum_k^{N_{\text{MM}}} \int d\mathbf{r} \frac{\rho_{\text{QM}}(\mathbf{r}) Q_k}{|\mathbf{r} - \mathbf{R}_k|} + \sum_A^{N_{\text{QM}}} \sum_k^{N_{\text{MM}}} \frac{Z_A Q_k}{|\mathbf{R}_A - \mathbf{R}_k|}, \quad (4)$$

where  $\rho_{\text{QM}}$  is the electron density and  $Z_A$  are effective nuclear charges of the QM region, and  $Q_k$  are classical electrostatic charges. van der Waals interactions in the second term,  $E_{\text{QM/MM}}^{\text{vdW}}$ , are represented in terms of a Lennard–Jones potential:

$$E_{\text{QM/MM}}^{\text{vdW}} = \sum_A^{N_{\text{QM}}} \sum_k^{N_{\text{MM}}} \epsilon_{\text{Ak}} \left[ \left( \frac{\sigma_{\text{Ak}}}{R_{\text{Ak}}} \right)^{12} - \left( \frac{\sigma_{\text{Ak}}}{R_{\text{Ak}}} \right)^6 \right]. \quad (5)$$

The above QM/MM description was deployed using the newly developed NWChem-AMBER interface (see Fig. 1), which builds on our extensible interface<sup>[92]</sup> for QM/MM simulations with

AMBER<sup>[6,7]</sup> and external QM programs. This interface allows us to integrate the vast array of electronic structure methods available in NWChem<sup>[5]</sup> including DFT, TD-DFT, and CC formulations with a classical description provided by AMBER. It should be noted that while the QM/MM partitioning results in a significant reduction in computational load, this alone is not always sufficient to provide a practical approach for simulations other than single point energy calculations. As a result for the optimization component of our calculations we have utilized a multiregion optimization strategy where optimizations of QM and MM regions are alternated.<sup>[93]</sup> During optimization of the MM region, the QM region is represented by a fixed electron density. The entire procedure contains the following steps:

1. Optimization of the QM subsystem keeping MM subsystem fixed.
2. Calculation of a reduced electrostatic representation for the QM subsystem.
3. Optimization of the MM subsystem keeping the QM subsystem fixed.
4. The procedure is repeated from steps 1 to 3 as a cycle until converged.

Note that in step 2, instead of employing the direct charge density  $\rho_{\text{QM}}$  resulting from the wavefunction recalculation which is computationally expensive, the ESP charge fitting scheme can be used. A set of ESP charges representing the QM subsystem are calculated and used in step 3 of MM optimization. This method greatly improves the efficiency of QM/MM calculations for large systems. Hence, eq. (4) for the MM optimization has a form:

$$E_{\text{QM/MM}}^{\text{electrostatics}} = \sum_i^{N_{\text{QM}}} \sum_k^{N_{\text{MM}}} \frac{Q_i Q_k}{|\mathbf{r}_i - \mathbf{r}_k|} \equiv E_{\text{ESP}}, \quad (6)$$

where  $Q_i$  represents the ESP fitted charge of QM atom  $i$ .

To define the aqueous solution model the chromophore (HBDI) was solvated within a 22 Å radius spherical droplet of classical triangulated water molecules (TIP3P model).<sup>[94]</sup> A soft half-harmonic potential was imposed beyond 22 Å radius from the model chromophore. The model chromophores were included in the QM subsystem and the water molecules were treated at the MM level. The VdW parameters for the chromophores were taken from the General AMBER Force Field (GAFF).<sup>[95]</sup>

All systems were initially optimized and equilibrated for 500 ps at 300 K using the PMEMD engine of the AMBER v16 code.<sup>[7]</sup> During the course of the MD equilibration, the chromophore was held fixed at the center of the water droplet. The equilibrated systems were optimized using the QM/MM multiregion optimization protocol described above. Mirroring gas phase calculations, the QM description at this step was based on a DFT/B3LYP/6-31G\* level of theory because forces are not yet available from the CR-EOMCCSD(T) methods. Following optimization, the excitation energies were calculated using CR-EOMCCSD(T) level of theory with the Def2-TZVP basis set.<sup>[85]</sup>

**Table 1.** Relative free energies of GFP model chromophores (kcal/mol).<sup>[a][b]</sup>

	Gas phase	Aqueous phase	
		Calculation	Experiment <sup>[c]</sup>
$\Delta G_{\text{cis} \rightarrow \text{trans}}^{\text{cat}}$	0.45	0.74	0.79
$\Delta G_{\text{cis} \rightarrow \text{trans}}^{\text{ani}}$	3.00	2.59	2.29
$\Delta G_{\text{cis} \rightarrow \text{trans}}^{\text{neu}}$	3.33	2.55	2.10
$\Delta G_{\text{cis} \rightarrow \text{trans}}^{\text{zwit}}$	1.03	3.59	n/a
$\Delta G_{\text{cis} \rightarrow \text{zwit}}^{\text{cat}}$	26.22	22.72	n/a
$\Delta G_{\text{neu} \rightarrow \text{zwit}}^{\text{cat}}$	23.91	23.76	n/a

[a] cat = cation; ani = anion; neu = neutral; zwit = zwitterion. [b] The estimate Gibbs energies are based on eq. (7). [c] Taken from Ref. 98.

To estimate relative stabilities of conformers, we used a procedure where solvation energies ( $E_{\text{solv}}$ ) were calculated using the self-consistent reaction field theory of Klamt and Schüürmann (COSMO).<sup>[96]</sup> The atomic radii were set at 1.172 for H, 1.576 for O, and 2.126 Å for N.<sup>[97]</sup> COSMO calculations were performed on QM/MM optimized structures with all the solvent removed. Thermal corrections of enthalpy ( $\Delta H$ ) and total entropies ( $S$ ) at 298.15 K were calculated using QM/MM vibrational calculations at DFT/B3LYP/6-31G\* level of theory. These were combined with CCSD internal QM ( $E_{\text{int}}^{\text{CCSD}}$ ) to arrive at the approximate values for relative free energies,

$$\Delta G = (\Delta E_{\text{int}}^{\text{CCSD}} + \Delta E_{\text{solv}}) + \Delta H - T\Delta S. \quad (7)$$

The calculated relative free energies are listed in the Table 1.

## Results and Discussion

### Cationic form

The optimized structures of the cationic *cis* and *trans* conformers in aqueous solution are shown in Figure 2. Overall, the presence of aqueous solution does not impact the structures in a significant way. The only discernible change is found for the *cis* conformer, which deviates from the planar structure of the *trans* conformer due to steric hindrance introduced by the nitrogen protonation. The angle between the phenol and the imidazolinone plane increases from ~16 to 19 degrees when going from gas to aqueous phase. For both conformers, we observe two water molecules coordinating the phenol OH group, and one water coordinating the NH group of imidazolinone. The imidazolinone ring oxygen in the *trans* conformer is more solvent exposed and has two coordinating waters, compared to one in the *cis* conformer. In gas phase the two conformers appear to have nearly the same ground state energies—at the CCSD level of theory the *cis* conformer is slightly more stable than the *trans* conformer by 0.45 kcal/mol. In solution, our QM/MM COSMO estimates show similar slight preference for the *cis* conformer by 0.74 kcal/mol. The result agrees well with the observed value of 0.79 kcal/mol reported by Tonge et al.<sup>[98]</sup> Overall, these numbers indicate that either conformer can be potentially accommodated in aqueous phase.



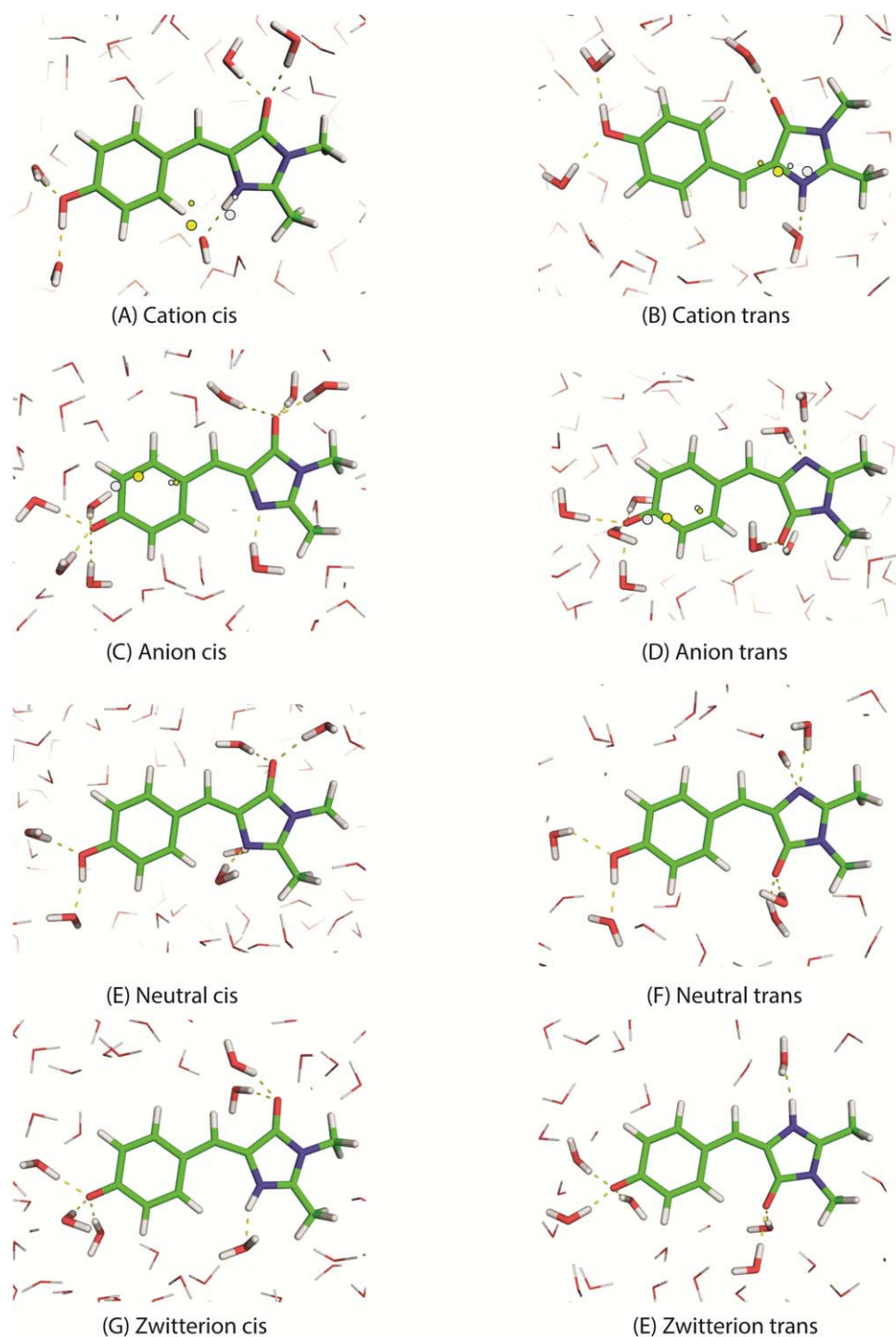


**Figure 2.** GFP model chromophore (HBDI) in water with different protonation states (*cis* and *trans* conformers). Carbon atoms are green, nitrogen atoms blue, oxygen atoms red, and hydrogen atoms white. For cationic and anionic forms, the large white and yellow circles represent the effective center of charge for the ground and excited states correspondingly. Small circles refer to the same quantities in the gas phase. [Color figure can be viewed at [wileyonlinelibrary.com](http://wileyonlinelibrary.com)]

In the gas phase, we calculate the absorption values to be 3.15 and 2.95 eV for *cis* and *trans* conformers, respectively. These values are in agreement with the experimental value of 3.05 eV<sup>[33]</sup> and in line with previous calculations using aug-MCQDPT2 (3.06 eV)<sup>[40]</sup> and XMCQDPT2 (3.12 eV).<sup>[50]</sup> For aqueous phase, we find that the *cis* conformer is characterized by the absorption value of 3.15 eV, and the *trans* conformer at

3.20 eV. Interestingly, both *cis* and *trans* absorption numbers agree with existing experimental data. In acidic aqueous solution (pH < 1), Andersen et al.<sup>[33,34]</sup> reported the maximum absorption of HBDI to be 3.13 eV. However, a slightly different absorption value of 3.17–3.20 eV<sup>[32,35]</sup> has been obtained by other groups. Looking at the differences between gas phase and aqueous values, we observe that they are sensitive to the

solute conformation. Indeed, for the *cis* conformer no difference is observed and for the *trans* conformer we notice a slight blue shift.

To gain further insight into the impact of an aqueous environment on the excited state properties of *cis* and *trans* conformers it is instructive to analyze the changes in charge distribution that occur on transfer to aqueous phase and during excitation. For charged systems, such as a cation or anion, a useful metric for such analysis can be found by defining an effective center of charge as a point where the dipole moment of the system (calculated at CCSD level of theory) vanishes. Given a total dipole ( $\mathbf{d}$ ) and charge of the system ( $Q$ ), it is given by

$$\mathbf{R}_c = \frac{\mathbf{d}}{Q}. \quad (8)$$

The location of this point for the cationic system is shown in Figure 2 (white/yellow circles), both for the unpolarized system (QM calculation at QM/MM geometry without inclusion of MM water molecules) and the fully polarized system (QM/MM calculation). In the ground state, the center of (overall positive) charge in both structures is near the NH bond on the imidazolinone ring, suggesting that this is the primary localization point of the electron hole in the system. Comparing the two conformers, it is evident that the center of charge is pushed further inside the molecule in the *trans* conformer. We observe that the impact of the aqueous environment is to pull the charge closer to the solvent boundary, which maximizes the solvation energy. Given the above mentioned difference between the two structures, the center of charge in the *cis* case is located much closer to the solvent compared to *trans*, which is consistent with the larger solvation energy that stabilizes the *cis* isomer. Transition to the excited state shifts the center of charge closer to the phenol group. Our calculations indicate that in the *trans* configuration, this move brings the electron hole to the area of higher (more positive) electrostatic potential, while the opposite is true for the *cis* configuration. This is consistent with the increased gap between the ground and excited state in the *trans* conformer.

### Anionic form

The optimized structures of the anionic state are also shown in Figure 2. The imidazolinone nitrogen is no longer protonated and we no longer have a twisting distortion in the *cis* conformer as observed in the cationic state. Other than a slight puckering in the *cis* conformer, which pulls the opposite ends of the molecule toward each other, the structural impact of aqueous solution remains small. This is consistent with previous QM/EFP calculations<sup>[62]</sup> of the related anionic form of DFHBDI chromophore where near planar structures formed the main population of the sampled structures. The anionic state exhibits much stronger solvent coordination than the cationic state. In both *cis* and *trans* conformers, we can identify four water coordinating phenol groups. The solvent accessibility of the imidazolinone nitrogen and oxygen depends on

the conformation, which impacts the coordination. For the *cis* conformer we observe one water interacting with a nitrogen and three waters interacting with an oxygen, and for the *trans* conformer both centers are coordinated by two waters. The CCSD gas phase calculations also indicate that the *cis* conformer is relatively more stable than the *trans* conformer by 3.0 kcal/mol. Similar situation persists in aqueous phase, where our estimates show the relative stability of the *cis* conformer at 2.6 kcal/mol. This is in line with the previously calculated value of 2.1 kcal/mol obtained using a combined CASSCF/EFP model,<sup>[61]</sup> and agrees well with the experimental value of 2.3 kcal/mol from Tonge et al.<sup>[98]</sup>

In the gas phase, several hypotheses have been put forward regarding the absorption value of the anionic form of the GFP chromophore. Measurements from action spectroscopy revealed the absorption peak at 2.59 eV.<sup>[33–35]</sup> Conversely, extrapolation from Kamlet–Taft fit by Dong et al.<sup>[32]</sup> suggested a more energetic absorption value of 2.84 eV. In addition, studies from photo-destruction spectroscopy propose the absorption value above 2.61 eV.<sup>[36]</sup> Our calculations show that in gas phase both conformers have absorption values at 2.70 eV. This falls squarely within the range of experimental values and is also consistent with previous calculations from CASPT2 (2.67 eV),<sup>[46]</sup> SA-CASSCF (2.69 eV),<sup>[48]</sup> and MRMP2 (2.61 eV)<sup>[42]</sup> approaches. To determine the effect of geometry on the absorption values, we have performed gas phase excitation energy calculations for anionic HBDI chromophores (both conformers) obtained from QM/MM optimizations. The absorption values for both conformers are estimated to be 2.65 eV, which is red-shifted from the gas phase optimized structure by  $-0.05$  eV. A similar red shift of  $-0.13$  eV in the absorption energy was reported in previous QM/EFP calculations<sup>[62]</sup> for the anionic DFHBDI.

Our calculations place the aqueous phase absorption values at 2.93 and 2.80 eV for the *cis* and *trans* conformers, respectively. Previous CASPT2 calculation of HBDI in water through PCM model estimated the absorption value for the *cis* conformer to be 2.69 eV.<sup>[39]</sup> Additional calculated absorption value of 2.86 eV was also reported for HBI model using CASPT2 method and explicit TIP3P water model.<sup>[51]</sup> Experimentally, the absorption spectrum for HBDI at high pH ( $> 11$ ) was measured to be 2.90–2.92 eV,<sup>[32–36]</sup> which agrees very well with our 2.93 eV calculated value for the *cis* conformer. Similar to the cationic state, the shift in absorption values is sensitive to the conformation, and these effects are amplified in the anionic state—the absorption energy increases by 0.23 eV in the *cis* conformer and by 0.1 eV in the *trans* conformer. This is in line with the increase of absorption value of 0.1 eV for DFHBDI in bulk aqueous phase as reported by Ghosh et al.<sup>[62]</sup> In addition, a very small solvent effect of polarization on the change of the excitation energy (0.03 eV) is suggested. Therefore, this supports the choice of nonpolarizable MM force field used in our study.

Performing the same charge analysis as we did for the cationic state, we observe that the center of negative charge is located on the phenol group side. Its position is not affected much by transition to the excited state, which is different to

Table 2. Calculated excitation energy (in eV) of the GFP model chromophores.

Chromophore	Gas			Water		
	TD-DFT	CR-EOMCCSD(T)	Experiment	TD-DFT	CR-EOMCCSD(T)	Experiment
Cation ( <i>cis</i> )	3.16	3.15 (3.47)	3.05 <sup>[a]</sup>	3.22	3.15 (3.46)	3.13–3.20 <sup>[b]</sup>
Cation ( <i>trans</i> )	3.18	2.95 (3.26)		3.29	3.20 (3.51)	
Anion ( <i>cis</i> )	3.09	2.70 (3.03)	2.59–2.84 <sup>[c]</sup>	3.18	2.93 (3.25)	2.90–2.92 <sup>[b]</sup>
Anion ( <i>trans</i> )	3.11	2.70 (3.03)		3.16	2.80 (3.12)	
Neutral ( <i>cis</i> )	3.45	3.69 (3.99)	3.35–3.65 <sup>[d]</sup>	3.37	3.43 (3.74)	3.33–3.35 <sup>[b]</sup>
Neutral ( <i>trans</i> )	3.39	3.61 (3.92)		3.40	3.39 (3.70)	
Zwitterion ( <i>cis</i> )	2.67	2.73 (3.06)	n/a	3.11	2.69 (3.01)	n/a
Zwitterion ( <i>trans</i> )	2.65	2.97 (3.31)	n/a	3.08	2.62 (2.94)	n/a

[a] Taken from Ref. 33. [b] Taken from Refs. 32–35. [c] Taken from Refs. 32–36. [d] Taken from Refs. 32,37,38. Numbers in the parentheses are based on EOMCCSD calculations.

what was observed for the cation. This indicates that excitation in the anionic case incurs little charge rearrangement. In both structures the transition to aqueous environment pulls the charge closer to the solvent. It also increases separation between the ground and excited state, particularly so in the *cis* case.

### Neutral form

The neutral form of the GFP model chromophore is characterized by a protonated phenol group. The optimized structures of both *cis* and *trans* conformers are shown in Figure 2. Similar to the anionic state, the structure of the *trans* conformer remains virtually unchanged on transfer to aqueous solution while the *cis* state exhibits slight puckering. We observe that the phenol OH group is coordinated by two water molecules in both *cis* and *trans* conformers. The coordination of the imidazolinone is very similar to that observed in the anionic state. The CCSD calculations suggest that the *cis* conformer of the neutral form of the GFP model chromophore is relatively more stable than the *trans* conformer by 3.3 kcal/mol. Our estimation in the aqueous phase also reveals similar *cis* conformer stability over the *trans* conformer by 2.55 kcal/mol. This is in line with the observed value of 2.1 kcal/mol from experiment.<sup>[98]</sup>

In the gas phase discrepancies between the maximum absorption of the neutral forms have been reported, from experiments. The extrapolation from a Kamlet–Taft fit suggests the absorption value at 3.51 eV.<sup>[32]</sup> The experiment using the charge group by Rajput et al. proposed the absorption at 3.35 eV.<sup>[37]</sup> Recently, Greenwood et al.<sup>[38]</sup> applied an alternative approach and reported the absorption value to be 3.65 eV. Our calculated absorption values are 3.69 and 3.61 eV for the *cis* and *trans* conformers, respectively, and seem to confirm to be within these measurements. Our numbers are also in line with previously calculated values of 3.71 eV (CAM-B3LYP)<sup>[38]</sup> and 3.58 eV (CASPT2)<sup>[60]</sup> for the *cis* conformer of HBDI.

In aqueous solution our calculated excitation energies of the neutral form were calculated to be 3.43 and 3.39 eV for the *cis* and *trans* isomers, respectively. These values are in good agreement with the experimentally measured absorption energy of 3.33–3.35 eV<sup>[32–35]</sup> for neutral pH solutions of the chromophore. Previous calculations by other groups have been

performed at the TD-DFT level using different model chromophores,<sup>[47,59]</sup> but no consensus has been reached. Xie and Zeng, using a combined explicit-implicit type model,<sup>[99,100]</sup> reported absorption values of 3.56 and 3.49 eV for the *cis* and *trans* conformers of HBMIA, respectively.<sup>[59]</sup> Conversely, Nemukhin et al., using a polarizable continuum model (PCM), estimated the absorption values for HBI at 2.74 (*cis*) and 2.84 eV (*trans*).<sup>[47]</sup> Additionally, the absorption peak of HBI from SA-2-CAS approach using Monte Carlo samples of the ground state chromophore in TIP3P water was reported to be 4.27 eV.<sup>[64]</sup>

### Zwitterionic form

In addition to the neutral form discussed above, a number of computational studies related to the zwitterionic form have been reported. The latter still carries net zero charge but instead of the phenol group the proton is now located on the imidazolinone nitrogen group. In gas phase, such a state is most certainly higher in energy than the neutral state. Our calculations show at the CCSD level of theory that the transfer of the proton from phenol to imidazolinone raises the energy by ~26 kcal/mol. There is little difference between the two conformations of the zwitter-ionic form. The *cis* conformer is slightly more stable than the *trans* conformer by 1.03 kcal/mol (CCSD). While the aqueous solution stabilizes the zwitterionic form, it remains ~20 kcal/mol above the neutral state.

In gas phase, our calculated absorption values of the zwitterionic HBDI are 2.73 and 2.97 eV for *cis* and *trans* conformers, respectively. These numbers are consistent with the previous calculated values in a range of 2.46–3.13 eV reported by Polyakov et al.<sup>[50]</sup> and with the calculations from post-HF and TD-DFT approaches reported for HBI and HBMIA.<sup>[54,58,59]</sup> In the aqueous phase we estimate absorption values of 2.69 and 2.62 eV for the zwitterionic form. This is in reasonable agreement with the observed absorption value of 2.55 eV reported for the zwitterionic form of the methoxyl derivative (pHBDIME+) species.<sup>[32]</sup> Previous calculations showing less agreement were based on the TD-DFT model and varied depending on the solvent treatment. PCM estimates<sup>[47]</sup> give values of 2.31 (*cis*) and 2.48 eV (*trans*) for the HBI model, and the combined explicit-implicit type model<sup>[99,100]</sup> of Xie and Zeng gives 3.33 eV for the *trans* form of HBMIA.<sup>[59]</sup> Overall, there seems to be no

compelling reason to assume that the zwitterionic form should contribute to the observed spectrum at neutral pH values.

## Conclusion

We have implemented QM/MM approach by combining NWChem and AMBER codes. This initial implementation is geared toward studies of aqueous systems allowing efficient optimization of large systems and calculations of excited state properties at various levels of theory. The interface has been tested through a systematic study of the photophysical properties for the GFP model chromophore analogue (HBDI) in aqueous phase using the high level QM method and explicit solvent treatment. Our calculations for the excitation energies of HBDI show good agreement with experimental data for both gas phase and aqueous environment. As indicated in Table 2, the performance of less computationally extensive TD-DFT methods is mixed at best, and a high level quantum-mechanical treatment appears to be essential to reliably capture variations of excited states across different protonation states and conformations. To fully approach experimental absorption numbers, inclusion of triples excitations is necessary. As Table 2 indicates, CR-EOMCCSD(T) leads to a sizable ( $\sim 0.3$  eV) correction to EOMCCSD numbers. The triples corrections, however, are uniform, which hints at the possibility of adding it as a postprocessing correction. The MM treatment of the solvent is clearly an approximation, but overall agreement with experimental aqueous absorption energies suggests that it may be sufficient to capture the essential features of the aqueous environment and its influence on excited states.

Our results show that impact of aqueous environment on cationic and anionic states generally results in blue shifts, that is, increase in the separation between ground and excited energy levels on solvation. The effect is much less pronounced in the cationic state. Center of charge analysis shows that the cationic state exhibits greater charge rearrangement during excitation than the anion. The absorption energy shifts on solvation are sensitive to the conformation of the chromophore. These effects can be rationalized based on charge movement into the area of higher/lower external electrostatic potentials, providing a potential pathway for control of GFP properties in the protein environment.

Our results indicate that at neutral pH levels the experimentally observed absorption signal of the GFP chromophore is most likely coming from the phenol protonated form of GFP. The other possibility suggested in previous works, a zwitterionic form, is higher in energy and does not match the experimental absorption data.

The presented results provide baseline and insights for further analysis of the GFP chromophore in protein matrix. Dealing with such a complex system within the QM/MM framework requires a treatment for bond crossing and better electrostatic description between QM and MM subsystems. In addition, more sophisticated free energy calculations are necessary. These effects will be taken into account in our future work to offer a more versatile QM/MM interface with

capabilities that encompass a vast array of simulations types for large complex systems.

**Keywords:** QM/MM · green fluorescent protein · Nwchem · AMBER · CCSD(T) · excited states · solvation

How to cite this article: T. Pirojsirikul, A. W. Götz, J. Weare, R. C. Walker, K. Kowalski, M. Valiev. *J. Comput. Chem.* **2017**, *38*, 1631–1639. DOI: 10.1002/jcc.24804

- [1] M. J. Field, P. A. Bash, M. Karplus, *J. Comput. Chem.* **1990**, *11*, 700.
- [2] H. M. Senn, W. Thiel, *Angew. Chem. Int. Ed.* **2009**, *48*, 1198.
- [3] U. C. Singh, P. A. Kollman, *J. Comput. Chem.* **1986**, *7*, 718.
- [4] A. Warshel, M. Levitt, *J. Mol. Biol.* **1976**, *103*, 227.
- [5] M. Valiev, E. J. Bylaska, N. Govind, K. Kowalski, T. P. Straatsma, H. J. J. Van Dam, D. Wang, J. Nieplocha, E. Apra, T. L. Windus, W. A. de Jong, *Comput. Phys. Commun.* **2010**, *181*, 1477.
- [6] R. Salomon-Ferrer, D. A. Case, R. C. Walker, *Wiley Interdiscip. Rev. Comput. Mol. Sci.* **2013**, *3*, 198.
- [7] D. A. Case, R. M. Betz, W. Botello-Smith, D. S. Cerutti, T. E. Cheatham, III, T. A. Darden, R. E. Duke, T. J. Giese, H. Gohlke, A. W. Götz, N. Homeyer, P. Janowski, J. Kaus, A. Kovalenko, T. S. Lee, S. LeGrand, P. Li, C. Lin, T. Luchko, R. Luo, B. Madej, D. Mermelstein, K. M. Merz, G. Monard, H. Nguyen, H. T. Nguyen, I. Omelyan, A. Onufriev, D. R. Roe, A. Roitberg, C. Sagui, C. L. Simmerling, J. Swails, R. C. Walker, J. Wang, R. M. Wolf, X. Wu, L. Xiao, D. M. York, P. A. Kollman, AMBER 2016; University of California: San Francisco, **2016**.
- [8] R. Y. Tsien, *Annu. Rev. Biochem.* **1998**, *67*, 509.
- [9] M. Zimmer, *Chem. Rev.* **2002**, *102*, 759.
- [10] R. M. Wachter, *Acc. Chem. Res.* **2007**, *40*, 120.
- [11] R. Heim, D. C. Prasher, R. Y. Tsien, *Proc. Natl. Acad. Sci. USA* **1994**, *91*, 12501.
- [12] C. W. Cody, D. C. Prasher, W. M. Westler, F. G. Prendergast, W. W. Ward, *Biochemistry* **1993**, *32*, 1212.
- [13] B. G. Reid, G. C. Flynn, *Biochemistry* **1997**, *36*, 6786.
- [14] D. P. Barondeau, C. J. Kassmann, J. A. Tainer, E. D. Getzoff, *Biochemistry* **2005**, *44*, 1960.
- [15] D. P. Barondeau, J. A. Tainer, E. D. Getzoff, *J. Am. Chem. Soc.* **2006**, *128*, 3166.
- [16] D. P. Barondeau, C. J. Kassmann, J. A. Tainer, E. D. Getzoff, *J. Am. Chem. Soc.* **2006**, *128*, 4685.
- [17] L. Zhang, H. N. Patel, J. W. Lappe, R. M. Wachter, *J. Am. Chem. Soc.* **2006**, *128*, 4766.
- [18] D. C. Prasher, V. K. Eckenrode, W. W. Ward, F. G. Prendergast, M. J. Cormier, *Gene* **1992**, *111*, 229.
- [19] N. P. Lemay, A. L. Morgan, E. J. Archer, L. A. Dickson, C. M. Megley, M. Zimmer, *Chem. Phys.* **2008**, *348*, 152.
- [20] S. R. Meech, *Chem. Soc. Rev.* **2009**, *38*, 2922.
- [21] A. Acharya, A. M. Bogdanov, B. L. Grigorenko, K. B. Bravaya, A. V. Nemukhin, K. A. Lukyanov, A. I. Krylov, *Chem. Rev.* **2017**, *117*, 758.
- [22] S. Kojima, H. Ohkawa, T. Hirano, S. Maki, H. Niwa, M. Ohashi, S. Inouye, F. I. Tsuji, *Tetrahedron Lett.* **1998**, *39*, 5239.
- [23] H. Niwa, S. Inouye, T. Hirano, T. Matsuno, S. Kojima, M. Kubota, M. Ohashi, F. I. Tsuji, *Proc. Natl. Acad. Sci. USA* **1996**, *93*, 13617.
- [24] M. V. Matz, A. F. Fradkov, Y. A. Labas, A. P. Savitsky, A. G. Zaraisky, M. L. Markelov, S. A. Lukyanov, *Nat. Biotechnol.* **1999**, *17*, 969.
- [25] R. Heim, A. B. Cubitt, R. Y. Tsien, *Nature* **1995**, *373*, 663.
- [26] R. M. Wachter, M.-A. Elsliger, K. Kallio, G. T. Hanson, S. J. Remington, *Structure* **1998**, *6*, 1267.
- [27] R. M. Wachter, B. A. King, R. Heim, K. Kallio, R. Y. Tsien, S. G. Boxer, S. J. Remington, *Biochemistry* **1997**, *36*, 9759.
- [28] W. W. Ward, H. J. Prentice, A. F. Roth, C. W. Cody, S. C. Reeves, *Photochem. Photobiol.* **1982**, *35*, 803.
- [29] A. F. Bell, X. He, R. M. Wachter, P. J. Tonge, *Biochemistry* **2000**, *39*, 4423.



- [30] A. F. Bell, D. Stoner-Ma, R. M. Wachter, P. J. Tonge, *J. Am. Chem. Soc.* **2003**, *125*, 6919.
- [31] K. Brejč, T. K. Sixma, P. A. Kitts, S. R. Kain, R. Y. Tsien, M. Ormö, S. J. Remington, *Proc. Natl. Acad. Sci. USA* **1997**, *94*, 2306.
- [32] J. Dong, K. M. Solntsev, L. M. Tolbert, *J. Am. Chem. Soc.* **2006**, *128*, 12038.
- [33] L. H. Andersen, A. Lapierre, S. B. Nielsen, I. B. Nielsen, S. U. Pedersen, U. V. Pedersen, S. Tomita, *Eur. Phys. J. D* **2002**, *20*, 597.
- [34] S. B. Nielsen, A. Lapierre, J. U. Andersen, U. V. Pedersen, S. Tomita, L. H. Andersen, *Phys. Rev. Lett.* **2001**, *87*, 228102.
- [35] M. W. Forbes, R. A. Jockusch, *J. Am. Chem. Soc.* **2009**, *131*, 17038.
- [36] K. Chingin, R. M. Balabin, V. Frankevich, K. Barylyuk, R. Nieckarz, P. Sagulenko, R. Zenobi, *Int. J. Mass Spectrom.* **2011**, *306*, 241.
- [37] J. Rajput, D. B. Rahbek, L. H. Andersen, T. Rocha-Rinza, O. Christiansen, K. B. Bravaya, A. V. Erokhin, A. V. Bochenkova, K. M. Solntsev, J. Dong, J. Kowalik, L. M. Tolbert, M. Axman Petersen, M. Brondsted Nielsen, *Phys. Chem. Chem. Phys.* **2009**, *11*, 9996.
- [38] J. B. Greenwood, J. Miles, S. D. Camillis, P. Mulholland, L. Zhang, M. A. Parkes, H. C. Hailes, H. H. Fielding, *J. Phys. Chem. Lett.* **2014**, *5*, 3588.
- [39] P. Altoe, F. Bernardi, M. Garavelli, G. Orlandi, F. Negri, *J. Am. Chem. Soc.* **2005**, *127*, 3952.
- [40] K. B. Bravaya, A. V. Bochenkova, A. A. Granovskii, A. V. Nemukhin, *Russ. J. Phys. Chem. B* **2008**, *2*, 671.
- [41] A. K. Das, J.-Y. Hasegawa, T. Miyahara, M. Ehara, H. Nakatsuji, *J. Comput. Chem.* **2003**, *24*, 1421.
- [42] E. Epifanovsky, I. Polyakov, B. Grigorenko, A. Nemukhin, A. I. Krylov, *J. Chem. Theory Comput.* **2009**, *5*, 1895.
- [43] V. Helms, C. Winstead, P. W. Langhoff, *J. Mol. Struct. THEOCHEM* **2000**, *506*, 179.
- [44] K. Kowalski, S. Krishnamoorthy, O. Villa, J. R. Hammond, N. Govind, *J. Chem. Phys.* **2010**, *132*, 154103.
- [45] T. Laino, R. Nifosi, V. Tozzini, *Chem. Phys.* **2004**, *298*, 17.
- [46] M. E. Martin, F. Negri, M. Olivucci, *J. Am. Chem. Soc.* **2004**, *126*, 5452.
- [47] A. V. Nemukhin, I. A. Topol, S. K. Burt, *J. Chem. Theory Comput.* **2006**, *2*, 292.
- [48] S. Olsen, S. C. Smith, *J. Am. Chem. Soc.* **2008**, *130*, 8677.
- [49] A. Petrone, P. Caruso, S. Tenuta, N. Rega, *Phys. Chem. Chem. Phys.* **2013**, *15*, 20536.
- [50] I. V. Polyakov, B. L. Grigorenko, E. M. Epifanovsky, A. I. Krylov, A. V. Nemukhin, *J. Chem. Theory Comput.* **2010**, *6*, 2377.
- [51] A. Sinicropi, T. Andruniow, N. Ferré, R. Basosi, M. Olivucci, *J. Am. Chem. Soc.* **2005**, *127*, 11534.
- [52] A. Toniolo, S. Olsen, L. Manohar, T. J. Martinez, *Faraday Discuss.* **2004**, *127*, 149.
- [53] O. Vendrell, R. Gelabert, M. Moreno, J. M. Lluch, *Chem. Phys. Lett.* **2004**, *396*, 202.
- [54] A. A. Voityuk, A. D. Kummer, M.-E. Michel-Beyerle, N. Rösch, *Chem. Phys.* **2001**, *269*, 83.
- [55] A. A. Voityuk, M.-E. Michel-Beyerle, N. Rösch, *Chem. Phys. Lett.* **1997**, *272*, 162.
- [56] A. A. Voityuk, M.-E. Michel-Beyerle, N. Rösch, *Chem. Phys.* **1998**, *231*, 13.
- [57] S. Wan, S. Liu, G. Zhao, M. Chen, K. Han, M. Sun, *Biophys. Chem.* **2007**, *129*, 218.
- [58] W. Weber, V. Helms, J. A. McCammon, P. W. Langhoff, *Proc. Natl. Acad. Sci. USA* **1999**, *96*, 6177.
- [59] D. Xie, J. Zeng, *J. Comput. Chem.* **2005**, *26*, 1487.
- [60] C. Filippi, M. Zaccheddu, F. Buda, *J. Chem. Theory Comput.* **2009**, *5*, 2074.
- [61] I. Polyakov, E. Epifanovsky, B. Grigorenko, A. I. Krylov, A. Nemukhin, *J. Chem. Theory Comput.* **2009**, *5*, 1907.
- [62] S. Bose, S. Chakrabarty, D. Ghosh, *J. Phys. Chem. B* **2016**, *120*, 4410.
- [63] K. Bhaskaran-Nair, M. Valiev, S. H. M. Deng, W. A. Shelton, K. Kowalski, X.-B. Wang, *J. Chem. Phys.* **2015**, *143*, 224301.
- [64] A. M. Virshup, C. Punwong, T. V. Pogorelov, B. A. Lindquist, C. Ko, T. J. Martinez, *J. Phys. Chem. B* **2009**, *113*, 3280.
- [65] K. B. Bravaya, B. L. Grigorenko, A. V. Nemukhin, A. I. Krylov, *Acc. Chem. Res.* **2012**, *45*, 265.
- [66] B. Mennucci, *Phys. Chem. Chem. Phys.* **2013**, *15*, 6583.
- [67] W. D. Cornell, P. Cieplak, C. I. Bayly, I. R. Gould, K. M. Merz, D. M. Ferguson, D. C. Spellmeyer, T. Fox, J. W. Caldwell, P. A. Kollman, *J. Am. Chem. Soc.* **1995**, *117*, 5179.
- [68] B. L. Grigorenko, A. V. Nemukhin, I. V. Polyakov, D. I. Morozov, A. I. Krylov, *J. Am. Chem. Soc.* **2013**, *135*, 11541.
- [69] K. B. Bravaya, M. G. Khrenova, B. L. Grigorenko, A. V. Nemukhin, A. I. Krylov, *J. Phys. Chem. B* **2011**, *115*, 8296.
- [70] S. Faraji, A. I. Krylov, *J. Phys. Chem. B* **2015**, *119*, 13052.
- [71] K. B. Bravaya, O. M. Subach, N. Korovina, V. V. Verkhusha, A. I. Krylov, *J. Am. Chem. Soc.* **2012**, *134*, 2807.
- [72] P. K. Gurunathan, A. Acharya, D. Ghosh, D. Kosenkov, I. Kaliman, Y. Shao, A. I. Krylov, L. V. Slipchenko, *J. Phys. Chem. B* **2016**, *120*, 6562.
- [73] P. Armengol, R. Gelabert, M. Moreno, J. M. Lluch, *J. Phys. Chem. B* **2015**, *119*, 2274.
- [74] V. R. I. Kaila, R. Send, D. Sundholm, *Phys. Chem. Chem. Phys.* **2013**, *15*, 4491.
- [75] C. Daday, C. Curutchet, A. Sinicropi, B. Mennucci, C. Filippi, *J. Chem. Theory Comput.* **2015**, *11*, 4825.
- [76] V. A. Mironov, K. B. Bravaya, A. V. Nemukhin, *J. Phys. Chem. B* **2015**, *119*, 2467.
- [77] M. S. Gordon, L. Slipchenko, H. Li, J. H. Jensen, In *Annual Reports in Computational Chemistry*; D. C. Spellmeyer, R. Wheeler, Eds.; Elsevier, Amsterdam, Netherlands, **2007**; pp. 177–193.
- [78] M. S. Gordon, D. G. Fedorov, S. R. Pruitt, L. V. Slipchenko, *Chem. Rev.* **2012**, *112*, 632.
- [79] P. Hohenberg, W. Kohn, *Phys. Rev. B* **1964**, *136*, 864.
- [80] W. Kohn, L. J. Sham, *Phys. Rev. A* **1965**, *140*, 1133.
- [81] R. G. Parr, W. Yang, *Density-Functional Theory of Atoms and Molecules*; Oxford University Press: New York, **1994**.
- [82] A. D. Becke, *J. Chem. Phys.* **1993**, *98*, 5648.
- [83] P. J. Stephens, F. J. Devlin, C. F. Chabalowski, M. J. Frisch, *J. Phys. Chem.* **1994**, *98*, 11623.
- [84] R. Ditchfield, W. J. Hehre, J. A. Pople, *J. Chem. Phys.* **1971**, *54*, 724.
- [85] F. Weigend, R. Ahlrichs, *Phys. Chem. Chem. Phys.* **2005**, *7*, 3297.
- [86] K. Kowalski, P. Piecuch, *J. Chem. Phys.* **2004**, *120*, 1715.
- [87] K. Kowalski, P. Piecuch, *J. Chem. Phys.* **2002**, *116*, 7411.
- [88] P. Piecuch, J. R. Gour, M. Wloch, *Int. J. Quantum Chem.* **2009**, *109*, 3268.
- [89] J. Geertsens, M. Rittby, R. J. Bartlett, *Chem. Phys. Lett.* **1989**, *164*, 57.
- [90] J. F. Stanton, R. J. Bartlett, *J. Chem. Phys.* **1993**, *98*, 7029.
- [91] P. Piecuch, J. A. Hansen, A. O. Ajala, *Mol. Phys.* **2015**, *113*, 3085.
- [92] A. W. Götz, M. A. Clark, R. C. Walker, *J. Comput. Chem.* **2014**, *35*, 95.
- [93] Y. Zhang, H. Liu, W. Yang, *J. Chem. Phys.* **2000**, *112*, 3483.
- [94] W. L. Jorgensen, J. Chandrasekhar, J. D. Madura, R. W. Impey, M. L. Klein, *J. Chem. Phys.* **1983**, *79*, 926.
- [95] J. Wang, R. M. Wolf, J. W. Caldwell, P. A. Kollman, D. A. Case, *J. Comput. Chem.* **2004**, *25*, 1157.
- [96] A. Klamt, G. Schüürmann, *J. Chem. Soc. Perkin Trans.* **1993**, *2*, 799.
- [97] E. V. Stefanovich, T. N. Truong, *Chem. Phys. Lett.* **1995**, *244*, 65.
- [98] X. He, A. F. Bell, P. J. Tonge, *FEBS Lett.* **2003**, *549*, 35.
- [99] J. Zeng, N. S. Hush, J. R. Reimers, *J. Chem. Phys.* **1993**, *99*, 1508.
- [100] N. S. Hush, J. R. Reimers, *Chem. Rev.* **2000**, *100*, 775.

Received: 1 February 2017

Accepted: 19 March 2017

Published online on 3 May 2017